IEEE Access
Multidisciplinary | Rapid Review | Open Access Journal

Received February 28, 2020, accepted March 9, 2020, date of publication March 13, 2020, date of current version March 24, 2020.

Digital Object Identifier 10.1109/ACCESS.2020.2980580

Coexistence and Performance Limits for the Cognitive Broadband Satellite System and mmWave Cellular Network

QIANFENG ZHANG[1], KANG AN[2], (Member, IEEE), XIAOJUAN YAN[1], (Member, IEEE), AND TAO LIANG[2]

[1]College of Mechanical, Naval Architecture and Ocean Engineering, Beibu Gulf University, Qinzhou 535011, China
[2]Sixty-Third Research Institute, National University of Defense Technology, Nanjing 210007, China

Corresponding author: Kang An (ankang89@nudt.edu.cn)

This work was supported in part by the Scientific Research Foundation of Beibu Gulf University under Grant 2019KYQD40, in part by the National Natural Science Foundation of China under Grant 61472094 and Grant 61901502, and in part by the Research Project of National University of Defense Technology (NUDT) under Grant ZK18-02-11.

ABSTRACT The application of millimeter wave (mmWave) spectrum for the next generation broadband communications has received significant attention recently. In this work, we investigate the performance limits for the coexistence of the geo-stationary orbit (GEO) broadband satellite networks and terrestrial mmWave cellular networks. Based on the assumption that the statistical channel state information (SCSI) is available at the terrestrial base station (BS), we propose a virtual uplink based transmit beamforming (BF) algorithm to maximize the ergodic capacity of the terrestrial user while satisfying the interference probability constraint of the satellite users. Furthermore, we derive the closed-form expressions for the outage probability (OP) and ergodic capacity (EC) of the terrestrial user. Besides, the asymptotic OP expression at high signal-to-noise ratio (SNR) is also developed in terms of diversity order and array gain of the terrestrial user. Finally, numerical results are given to confirm the validity of the proposed BF scheme and theoretical derivations, and reveal the impact of key parameters on the performance of the terrestrial user coexisting with the multiple satellite users.

INDEX TERMS Cognitive radio, millimeter wave, transmit beamforming, satellite communication, cellular network, performance analysis.

I. INTRODUCTION

Satellite communication (SATCOM) has been widely applied in many fields, such as navigation, broadcasting, rescue, and disaster relief, since it can overcome long distances and inhospitable terrains, as well as provide wide coverage and high data rate for worldwide users [1], [2]. For current satellite communication systems, such as Inmarsat, Globalstar and Iridium, mobile satellite service (MSS) are often achieved in the low frequency bands below 10 GHz. To accommodate the increasing traffic demands in the future, the research on higher frequency band, such as millimeter wave (mmWave) satellite communications have been accelerated in both of the academic and industry communities. Moreover, according to the International Telecommunication Union (ITU) regulations, the mmWave will be the main spectral band in future satellite networks to achieve the seamless broad band access wherever the terrestrial deployment cannot be provided or cost unfavorable [3].

The remarkable success of wireless technologies has led to an insatiable demand for mobile data over past decades. Emerging demand for high-speed reliable communications with significantly improved user experience has been driving the development of the fifth generation (5G) cellular networks [4], [5]. More recently, the framework of hybrid satellite terrestrial networks, which jointly exploit advantages of both systems [6]–[8], has been viewed as a promising candidate for the future 5G infrastructures [9], [10]. Due to the huge amount of potential spectrum and superiority in offering magnitude increase in system capacity, millimeter wave has been considered as one of the most promising candidate for the next generation communications. One of

The associate editor coordinating the review of this manuscript and approving it for publication was Wei Feng.

the candidate bands for the deployment of mmWave cellular mobile networks is the portion of spectrum between 20 and 90 GHz [4], [5].

However, due to the constantly expanding demand of multimedia services, it is foreseeable that the spectrum congestion in millimeter wave will also inevitably become the crucial challenge for both satellite and terrestrial communications in future wireless networks [11], [12]. In this regard, it has become a critical issue to explore new techniques to address the spectrum scarcity in wireless communications. Recently, cognitive radio (CR) has been considered as one of the promising approaches to improve the spectrum efficiency [13]. Many standard groups and researchers have focused on the application of CR techniques in satellite and terrestrial networks, which constitutes a new architecture termed as cognitive satellite terrestrial network (CSTN) [14]–[16]. In this network, the satellite network is termed as a primary/secondary network (PN/SN), shares the radio spectrum and coexists with the terrestrial network, which corresponding to the SN/PN. To accomplish this, the SN often employs power control or transmit beamforming (BF) to ensure the imposed interference to the authorized user is below a predefined threshold [15], [16].

For example, with single antenna deployed at the cognitive terrestrial BS, a power allocation scheme and the impact of the spatial distribution of primary transmitters on the cognitive networks were studied in [17]. In [18], the authors studied the outage performance of CSTN with interference temperature constraint at the primary satellite user. Besides, the author of [19] investigated the effects of practical hardware impairments on a CSTN with the constraints of both spectrum efficiency and reliability. In [20], the authors analyzed the cognitive zone in broadband satellite communication systems by employing a blind and link-based approaches. Moreover, to take full advantage of the multiple antennas techniques in the CSTN, the authors of [21] derived the ergodic capacity (EC) expression for by assuming that the BS was deployed with a uniform linear array (ULA) and maximal ratio transmission (MRT) is used as the transmit BF scheme. The work of [22] studied the performance of cognitive fixed satellite service (FSS), where the effect of BS location and antenna configurations on the interference level at the FSS was analyzed. In [23], a cooperative scheduling algorithm for the coexistence of FSS and terrestrial cellular networks was proposed based on a game theoretical framework. Considering a more general scenario, i.e., a CSTN with multiple users, the authors of [24] proposed two transmit BF schemes, namely, linearly constrained minimum variance (LCMV) and second order cone programming (SOCP) to maximize the signal-to-interference-plus-noise ratio (SINR) of the desired terrestrial user while minimizing the interference towards the primary user.

Although these prior works such as [17]–[24] have greatly improved our understanding on the coexistence of satellite networks and terrestrial cellular systems, it should be pointed out that they were merely obtained through system level Monte Carlo simulations, which actually are not only computationally inefficient but also mathematically intractable. Besides, the authors only analyzed the interference level at the satellite users, whereas the key performance merits of the terrestrial cellular user, which are very useful in understanding the performance limits and the potential application of CR techniques, remains unreported. Meanwhile, compared with ULA, since uniform planar array (UPA) can control the radiation pattern in both vertical and horizontal dimensions [25], [26], it can provide higher beam gain and enhanced interference suppression capability with compact structure in mmWave. However, the BF schemes for UPA is still an interesting yet challenging topic. These observations motivate the work of this paper. To summary, the detailed contributions are outlined as follows:

- We consider a general frame work for the cognitive satellite terrestrial network, where a GEO satellite network serving multiple users, shares the downlink spectrum and coexists with a terrestrial mmWave cellular network. Here, many ITU recommendations and other standards are adopted to establish the mmWave channel, antenna and pathloss models. It is worth-mentioning that our work includes the system models in [17]–[20] as a special case, where only one satellite user is considered.
- By supposing that the BS is deployed with a UPA, we first formulate a constrained optimization problem to maximize the ergodic capacity of the terrestrial user while satisfying the interference probability constraint of the satellite users. Then, we employ the available statistical channel state information (SCSI) at BS, and propose a virtual uplink based beamforming scheme to solve the optimization problem, which can obtain the analytical expressions of beamforming weight vector and power coefficient. Our work extends the previous works with BS employing a single antenna in [17]–[20], and an ULA in [21]–[24] to a more general case.
- We derive analytical expressions for the outage probability and ergodic capacity of the terrestrial user, based on which the effect of various key parameters on the system performance with BS employing the proposed transmit BF algorithm can be revealed. To gain further insight, simple asymptotic OP expression at high SNR regime with respect to the diversity order and array gain are developed to show the asymptotic behavior of the terrestrial network. To the best of our knowledge, this is the first time that such analytical expressions are developed for performance analysis of cognitive satellite terrestrial networks in mmWave scenario.

The rest of this paper is organized as follows. In Section II, we describe the system model of the cognitive broadband satellite and terrestrial cellular network in mmWave scenarios. In Section III, we formulate a constrained optimization problem and propose the virtual uplink based BF method to obtain the analytical weight vectors and transmit power coefficient. In Section IV, we analyze the statistical properties of satellite and terrestrial links in mmWave scenario.

In section V, we derive analytical expressions of outage probability, ergodic capacity, and asymptotic result at high SNR for the terrestrial user. Numerical results and discussion are given in Section VI. Finally, our conclusions are drawn in Section VII.

Notation: $E[\cdot]$ denotes the expectation operator, $|\cdot|$ the absolute value, $\max(\cdot)$ and $\min(\cdot)$ the maximum and minimum values, and $\exp(\cdot)$ the exponential function, $\mathcal{N}_C(m, \sigma^2)$ the complex Gaussian distribution with mean m and variance σ^2. $G_{p,q}^{m,n}[\cdot|\cdot]$ is the Meijer-G functions with a single variable [42], and $G_{1,[1:1],0,[1:1]}^{1,1,1,1,1}[\cdot|\cdot]$ is the Meijer-G functions of two variables [44].

II. SYSTEM MODEL

We consider a cognitive scenario as shown in Fig. 1, where a broadband satellite network and a terrestrial cellular network, termed as primary network (PN) and secondary network (SN), respectively, coexist with each other and share the same downlink spectral resource. Here, the PN consists of a GEO satellite (SAT) and K primary users (PUs) denoted as PU_k ($k \in \mathcal{K} = \{1, 2, \ldots, K\}$), while the SN contains a multi-antenna base station (BS) and a secondary user (SU). It is different from most of the previous cognitive satellite terrestrial model in [17]–[24], because we suppose that the satellite serves multiple users simultaneously and the BS is employed with an UPA.[1] Next, we will introduce the different submodels.

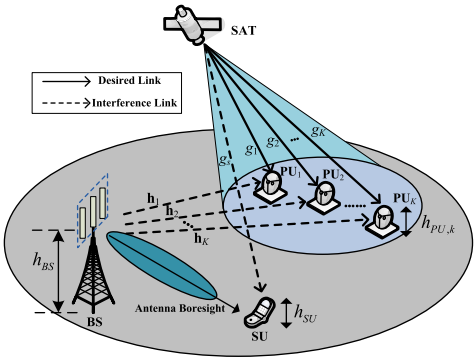

FIGURE 1. System model.

A. ANTENNA MODEL

In mmWave broadband satellite communications, the SAT often employs direct radiating arrays or array-fed reflector antennas. According to [1], the beam gain of SAT antenna can be well-modeled with Bessel function as

$$G_t^S(\varphi) = G_{t,max}^S \left(\frac{J_1(u)}{2u} + 36\frac{J_3(u)}{u^3} \right)^2, \tag{1}$$

with

$$u = 2.07123 \frac{\sin\varphi}{\sin\varphi_{3dB}}, \tag{2}$$

[1] In this paper, we assume that power amplify nonlinearity can be perfectly mitigated, the adverse impact of power amplify nonlinearity [27] on the considered network will be the work in our future research.

where $G_{t,max}^S$ represents the maximum beam gain at the on-board antenna boresight, φ the angle between the receiver and the beam center with respect to the satellite, and φ_{3dB} the 3-dB beamwidth.

By considering that the directional parabolic antenna is commonly adopted at the satellite receivers, the antenna gain of PU is approximated as

$$G_r^S(\beta)[dB] = \begin{cases} G_{r,\max}^S, & for\ 0^\circ < \beta \le 1^\circ \\ 32 - 25\log\beta, & for\ 1^\circ < \beta < 48^\circ \\ -10, & for\ 48^\circ < \beta < 180^\circ, \end{cases} \tag{3}$$

where $G_{r,\max}^S$ is the maximum beam gain at the boresight, and β the off-boresight angle of corresponding receiver. In satellite communications, since the k-th PU often points to the SAT, namely, $0^\circ < \beta_{p,k} < 1^\circ$, we have $G_r^P(\beta_{p,k}) = G_{r,\max}^B$. While for the BS-$\text{PU}_k$ interference link, $\beta_{s,k}$ can be calculated as [28]

$$\beta_{s,k} = \arccos\left(\cos(\alpha_k)\cos(\varepsilon_k)\cos(\vartheta_k) + \sin(\alpha_k)\sin(\varepsilon_k)\right), \tag{4}$$

where ϑ_k and α_k are the azimuth angle and elevation angle with respect to the PU, respectively, and ε_k can be given by

$$\varepsilon_k = \frac{h_{BS} - h_{PU}}{d_{sp,k}} - \frac{d_{sp,k}}{2r_e}, \tag{5}$$

where h_{BS} and h_{PU_k} are the antenna heights of the BS and PU_k in meters, respectively, $d_{sp,k}$ the distance between BS and PU_k, and r_e the earth radius.

Most of these aforementioned works employed the ULAs at BS, without taking full advantage of the vertical dimension. Thus, in mmWave scenario, array structures are expected to be implemented in two-dimensional UPAs to improve the received signal quality and simultaneously suppress the interference effectively [25]. As shown in Fig. 2, the BS is equipped with a $N_h \times N_v$ sized UPA, where there has N_h columns with each having N_v elements, spaced by d_h and d_v, respectively. In this array, each antenna port constitutes of a linear array with N_v vertical elements, which are excited with

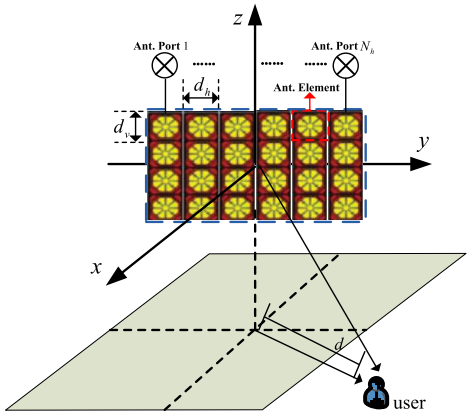

FIGURE 2. Planar antenna array structure.

the proper amplitudes and phases in analog domain. Thus, the main beam tilting angle of each antenna port is steered to the same fixed value ϕ_{tilt} according to the mean value of the vertical angle of the users [26]. Thus, the radiation pattern of each port in dB can be formulated as [25], [26],

$$G_t^B(\theta,\phi) = G_{\max}^B - \min\{A(\theta,\phi), A_m\} \overset{(a)}{=} g_{\max}^B g(\theta,\phi), \quad (6)$$

where (a) denotes the logarithm contrary transformation with $g_{\max}^B = 10^{(G_{\max}^B/10)}$, and $g(\theta,\phi) = 10^{(-A(\theta,\phi)/10)}$. In (6), θ and ϕ represent, respectively, the horizontal angle and vertical angle of the user, $G_{\max}^B$ the maximum antenna gain at the boresight direction, which can be calculated as

$$G_{\max}^B = \frac{4\pi}{\int\int g(\theta,\phi)\, d\Omega} d\theta d\phi, \quad (7)$$

with $d\Omega$ being the solid angle, and $A(\theta,\phi)$ is computed as

$$A(\theta,\phi) = A_H(\theta) + A_V(\phi), \quad (8)$$

where $A_H(\theta)$ and $A_V(\phi)$ are the horizontal and vertical beampatterns given by [29]

$$A_H(\theta) = \min\left\{12\left(\frac{\theta}{\theta_{3dB}}\right), A_m\right\}, \quad (9)$$

$$A_V(\phi) = \min\left\{12\left(\frac{\phi-\phi_{tilt}}{\phi_{3dB}}\right), SLA_V\right\}, \quad (10)$$

where A_m is the frontback ratio, and SLA_V the side-lobe level limit. Besides, θ_{3dB} and ϕ_{3dB} are the $3dB$ beamwidth of the horizontal and vertical patterns, respectively. As shown in Figs. 3 and 4, let x, y and Δz denote the relative distance between the BS UPA center and the user x-axis, y-axis and z-axis, we have

$$\theta = \arctan\frac{y}{x}, \quad \phi = \arctan\frac{\Delta z}{\sqrt{x^2+y^2}}. \quad (11)$$

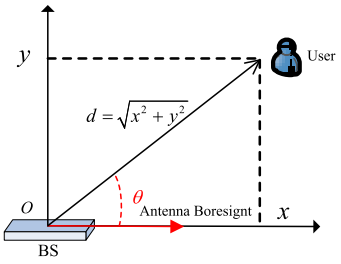

FIGURE 3. Diagram of a receiver's horizontal angles.

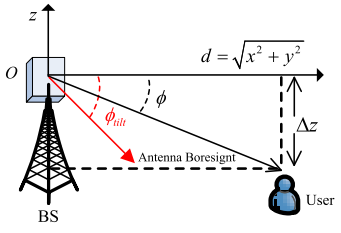

FIGURE 4. Diagram of a receiver's elevation angles.

B. CHANNEL MODEL

The emerging interest in provisioning broadband and multimedia services from satellite networks has resulted in the application of higher frequency bands above 10 GHz, such as Ka (20-30GHz) and Q/V (40-50GHz) bands, where the impact of atmosphere attenuation should be taken into account. Among the various atmosphere fading effects, the rain attenuation is the dominate factor, which is modeled as the log-normal fading distribution based on the state-of-art empirical model [1]. The resulting distribution of the channel gain in dB, $\xi_{gdB} = 20\log_{10}\left(|\xi_g|^2\right)$ can be expressed as

$$\ln\left(\xi_{gdB}\right) \sim \mathcal{N}_C(\mu,\nu), \quad (12)$$

where μ and ν represent the log-normal location and scale parameters, respectively. The corresponding channel rain fading coefficient is given by

$$g = \xi_g^{-\frac{1}{2}} e^{-j\zeta}, \quad (13)$$

where ζ denotes the phase coefficient uniformly distributed over $[0, 2\pi)$, ξ_g is the distribution of the power gain.

The mmWave channels are characterized by a sparse set of multipath components because of its limited scattering. In terrestrial cellular networks, the sparse scattering model is commonly used to describe the mmWave channel [5], [22], [23]. Without loss of generality, the channel vectors of BS-SU, and BS-PU$_k$ links, namely, $\mathbf{h}_s$ and $\mathbf{h}_k$ can be mathematically expressed as

$$\mathbf{h}_s = \sqrt{\frac{N_h}{L_s}} \sum_{l=1}^{L_s} \sqrt{g\left(\theta_{s,l},\phi_{s,l}\right)} \rho_{s,l} \mathbf{a}_s\left(\theta_{s,l}\right), \quad (14)$$

$$\mathbf{h}_k = \sqrt{\frac{N_h}{L_k}} \sum_{l=1}^{L_k} \sqrt{g\left(\theta_{k,l},\phi_{k,l}\right)} \rho_{k,l} \mathbf{a}_k\left(\theta_{k,l}\right), \quad (15)$$

where L_s and L_k represent the numbers of multi-path signals, $\rho_{s,l}$ and $\rho_{k,l}$ the fading coefficients, $E[\rho_{s,l}] = E\left[\rho_{k,l}\right] = 0$ and $E[|\rho_{s,l}|^2] = E[|\rho_{k,l}|^2] = 1$. $(\theta_{s,l},\phi_{s,l})$ and $(\theta_{k,l},\phi_{k,l})$ are the angle-of-departures (AODs) of the l-th path signal, respectively. The steering vectors $\mathbf{a}_s(\theta_{s,l})$ and $\mathbf{a}_k(\theta_{k,l})$ can be written as

$$\mathbf{a}_s\left(\theta_{s,l}\right) = \frac{1}{\sqrt{N_h}}\left[\exp\left(j\kappa i D\sin\theta_{s,l}\right)\right]_{i\in\mathcal{I}(n)}^T, \quad (16)$$

$$\mathbf{a}_k\left(\theta_{k,l}\right) = \frac{1}{\sqrt{N_h}}\left[\exp\left(j\kappa i D\sin\theta_{k,l}\right)\right]_{i\in\mathcal{I}(n)}^T, \quad (17)$$

where the steered vectors $\mathbf{a}_s(\theta_{s,l})$ and $\mathbf{a}_k(\theta_{k,l})$ respectively represent the discrete and complex spatial sinusoid corresponding to a point source in the relevanted AODs. $\mathcal{I}(n) = \{\ell - (N_h-1)/2\}, (\ell = 0, 1, \ldots N_h - 1)$, is a symmetric set of indices centered around 0, and κ denotes the wavenumber. Consequently, by employing (14) and (15), the non-negative definite Hermitian channel correlation matrix (CCM) of $\mathbf{h}_s$

and $\mathbf{h}_k$ can be, respectively, calculated as [30]

$$\mathbf{R}_s = E\left[\mathbf{h}_s\mathbf{h}_s^H\right] = \frac{1}{L_s}\sum_{l=1}^{L_s} g\left(\theta_{s,l},\phi_{s,l}\right)\mathbf{a}_s\left(\theta_{s,l}\right)\mathbf{a}_s^H\left(\theta_{s,l}\right), \tag{18}$$

$$\mathbf{R}_k = E\left[\mathbf{h}_k\mathbf{h}_k^H\right] = \frac{1}{L_k}\sum_{l=1}^{L_k} g\left(\theta_{k,l},\phi_{k,l}\right)\mathbf{a}_k\left(\theta_{k,l}\right)\mathbf{a}_k^H\left(\theta_{k,l}\right). \tag{19}$$

C. PATHLOSS MODEL

The common mmWave statistical model describing the average path loss (not including small-scale fading) in urban cellular networks without line-of-sight (LOS) can be given by [31]

$$L_{ss}\left(d_s\right)[dB] = \xi + 10\beta\log_{10}\left(d_s\right) + \chi, \tag{20}$$

where d_s is the distance between the BS and SU, ξ and β the linear model parameters and χ accounting for variances in shadowing fading. According to the ITU recommendation [32], the standard model of terrestrial interference link is

$$L_{sp,k}(d_{sp,k})[dB] = 32.5 + 20\log(f_c) + 20\log_{10}(d_{sp,k}) + A_h, \tag{21}$$

where f_c denotes the carrier frequency, $d_{sp,k}$ the distance from BS to PU_k, and A_h the clutter loss given by

$$A_h = 10.25e^{-d_n}F_{f_c}\left[1-\tanh\left[6\left(\frac{h_{PU}}{h_a}\right)-0.625\right]\right]-0.33, \tag{22}$$

with d_n and h_a being the nominal distance and nominal height, and

$$F_{f_c} = 0.25 + 0.375\{1+\tanh[7.5(f_c-0.5)]\}. \tag{23}$$

According to the Friis' Law for free-space propagation, the path loss for satellite links (scaled in dB) relative to a frequency band is assumed to have a linear dependence with logarithmic distance as

$$L\left(d\right)[dB] = 20\log_{10}\left(\frac{c}{4\pi f_c d}\right), \tag{24}$$

where c is the propagation speed. Since the distance between two receivers is much smaller than that of the satellite altitude, for the sake of simplicity, the relative distance d can be supposed to be the GEO elevation distance [33].

D. RECEIVED SIGNAL MODEL

As shown in Figs. 1 and 2, when the SAT works in broadcast mode and transmits the signal $s(t)$ obeying $E[|s\left(t\right)|^2] = 1$ to the K PUs, and simultaneously, BS transmits the signal $x(t)$ satisfying $E[|x\left(t\right)|^2] = 1$ to the SU with the same frequency after performing BF at the antenna ports with weight vector $\mathbf{w} \in \mathbb{C}^{N\times 1}$ and , the received signals at PU_k and SU can be, respectively, expressed as

$$y_{p,k}(t) = \underbrace{\sqrt{P_s G_t^{\mathrm{S}}(\varphi_k)G_r^{\mathrm{P}}(\beta_{p,k})L_{p,k}}g_k s\left(t\right)}_{\text{signal}} + \underbrace{\sqrt{P_b g_{\max\mathrm{B}} G_r^{\mathrm{P}}(\beta_{s,k})L_{sp,k}}\mathbf{w}^H\mathbf{h}_k x\left(t\right)}_{\text{interference}} + n_k(t), \tag{25}$$

and

$$y_s\left(t\right) = \underbrace{\sqrt{P_b g_{\max\mathrm{B}} L_s}\mathbf{w}^H\mathbf{h}_s x\left(t\right)}_{\text{signal}} + \underbrace{\sqrt{P_s G_t^{\mathrm{S}}(\varphi_s)L_{ps}}g_s s\left(t\right)}_{\text{interference}} + n_s\left(t\right), \tag{26}$$

where P_s and P_b denote the transmit powers at the SAT and BS, $n_s\left(t\right)$ and $n_k\left(t\right)$ the zero mean additive white Gaussian noise (AWGN) at SU and PU_k satisfying $n_s\left(t\right) \sim \mathcal{N}_C\left(0,\sigma_s^2\right)$ and $n_k\left(t\right) \sim \mathcal{N}_C\left(0,\sigma_k^2\right)$, respectively. $G_t^S(\varphi_k)$ and $G_t^S(\varphi_s)$ can be obtained via (1), $G_r^P(\beta_{p,k})$ and $G_r^P(\beta_{s,k})$ have given by (3), and pathloss of each link can be corresponding computed through (20), (21) and (24).

Based on (25) and (26) along with some necessary manipulations, the output SINR of the SU can be written as

$$\gamma_s = \frac{P_{R,s}}{P_{I,s}+\sigma_s^2}, \tag{27}$$

where $P_{R,s} = P_b\bar{L}_s\left|\mathbf{w}^H\mathbf{h}_s\right|^2$ and $P_{I,s} = P_s\bar{L}_{ps}\left|g_s\right|^2$ with $\bar{L}_s = L_s G_t^B(\theta_s,\phi_s)$ and $\bar{L}_{ps} = L_{ps}G_t^S(\varphi_s)$. The output SINR of PU_k can be given by

$$\gamma_{p,k} = \frac{P_{R,k}}{P_{I,k}+\sigma_k^2}, \tag{28}$$

where $P_{R,k} = P_s\bar{L}_p\left|g_k\right|^2$ and $P_{I,k} = P_b\bar{L}_{sp,k}\left|\mathbf{w}^H\mathbf{h}_k\right|^2$ with $\bar{L}_p = G_t^S(\varphi_k)G_r^S(\beta_{p,k})$ and $\bar{L}_{sp,k} = G_t^B(\theta_k,\phi_k)G_r^S(\beta_{s,k})$.

In what follows,we will propose a transmit BF scheme to maximize the ergodic capacity of SU while satisfying the interference probability constraint at PUs, and analyze the performance of SU with respect to different key merits.

III. COEXISTENCE DESIGN

In this section, we focus on the digital BF scheme for the array formed by N_h antenna ports, which has been shown in Fig. 2 and discussed in Section II-B. Our objective is to maximize the ergodic capacity of the SU while satisfying the interference probability constraint of each PU.[2] To this end, we formulate a constrained optimization problem to

[2]The interference probability constraint is commonly used in spectrum sharing environment to ensure that the outage level caused by unacceptable mutual interference is no more than a certain percentage of time [16], [34].

implement the transmit BF and power control at BS, namely,

$$\max_{P_b,\mathbf{w}} E[\log_2(1+\gamma_s)], \tag{29a}$$
$$s.t.\ \min\left\{\Pr\left(P_{I,k}\le Q_k\right)\right\}\ge 1-p_{out}, \tag{29b}$$
$$s.t.\ \ \|\mathbf{w}\|_F^2=1, P_b\le P_{\max}, \tag{29c}$$

where P_{max} denotes the maximum allowable transmit power at the BS, Q_k the interference threshold at the k-th PU, and $p_{out}\in(0,1]$ the interference constraint threshold.

Limited by the fast fading, training sequence, and heavy feedback burden, instantaneous CSI is difficult to obtain in practice and statistical CSI (SCSI) is a choice worthy of consideration due to its advantage of low implementation complexity [35]. Under this condition, we suppose that BS has the SCSIs of the BS-SU and BS-PU links, which means that the $\mathbf{R}_s$ and $\mathbf{R}_k$ respectively given in (18) and (19) are known at the BS. Due to the fact that $\mathbf{h}_k\sim\mathcal{N}(\mathbf{0},\mathbf{R}_k)$, the interference probability for k-th PU in (29b) can be given by

$$\begin{aligned}\Pr(P_{I,k}\le Q_k)&=1-\exp\left(-\frac{Q_k}{P_b\bar{L}_{sp,k}\mathbf{w}^H\mathbf{R}_k\mathbf{w}}\right)\\&\ge 1-p_{out}.\end{aligned} \tag{30}$$

In deriving (30), we have applied the fact that $\mathbf{w}^H\mathbf{h}_k\mathbf{h}_k^H\mathbf{w}$ follows the exponential distribution with covariance $\mathbf{w}^H\mathbf{R}_k\mathbf{w}$ [14]. Substituting (30) into (29b) yields the probability constraint as

$$P_b\bar{L}_{sp,k}\ln\left(\frac{1}{p_{out}}\right)\mathbf{w}^H\mathbf{R}_k\mathbf{w}\le Q_k. \tag{31}$$

By employing the Jensen inequality $E\left[\log_2\left(1+\gamma_s\right)\right]\le\log_2\left(1+E\left[\gamma_s\right]\right)$, and the identity $E\left[\left|\mathbf{w}^H\mathbf{h}_s\right|^2\right]=\mathbf{w}^H\mathbf{R}_s\mathbf{w}$, (29) can be rewritten as

$$\max_{P_b,\mathbf{w}} P_b\mathbf{w}^H\mathbf{R}_s\mathbf{w}, \tag{32a}$$
$$s.t.\ P_b\bar{L}_{sp,k}\ln\left(\frac{1}{p_{out}}\right)\mathbf{w}^H\mathbf{R}_k\mathbf{w}\le Q_k,\quad k\in\mathcal{K}=\{1,2,\ldots,K\} \tag{32b}$$
$$s.t.\ \ \|\mathbf{w}\|_F^2=1, P_b\le P_{\max}. \tag{32c}$$

Different to those who solve above problem by using relaxation techniques and standard optimization packages, by employing the downlink-uplink duality, we derive a new algorithm to obtain the analytical BF weight vectors $\mathbf{w}$ and transmit power coefficient p_b as follows.

From (32), we can see that if selecting the normalized BF weight vector $\mathbf{w}$ to maximize the $\mathbf{w}^H\mathbf{R}_s\mathbf{w}$ and simultaneously minimize the $\mathbf{w}^H\mathbf{R}_k\mathbf{w}$, $\forall k\in\mathcal{K}$, the objective function will be maximized. That is to say, the beam pattern generated by $\mathbf{w}$ should focus on the direction of SU and null the direction of those K PUs [36]. Therefore, we propose the ideal of virtual uplink BF scheme to solve the optimization problem in (32). Specifically, by supposing that SU and the k-th PU transmit $x^u(t)$ and $s_k^u(t)$ to BS with the power $P_{\max}$, respectively, and the virtual uplink fading channel vectors of SU-BS and PU$_k$-BS links are supposed to be similar with those of downlink, namely, $\mathbf{h}_s$ and $\mathbf{h}_k$, the virtual output signal at the BS after uplink BF with weight vector $\tilde{\mathbf{w}}$ is

$$\begin{aligned}y_s^u(t)=\tilde{\mathbf{w}}^H\underbrace{\sqrt{P_{\max}\bar{L}_s}\mathbf{h}_s x^u(t)}_{\text{signal}}\\+\tilde{\mathbf{w}}^H\underbrace{\sqrt{P_{\max}}\sum_{k=1}^{K}\sqrt{\bar{L}_{sp,k}}\mathbf{h}_k s_k^u(t)+n_s(t)}_{\text{interference+noise}}.\end{aligned} \tag{33}$$

The received power of the interference-plus-noise at the BS can be given by

$$\begin{aligned}P_{I+N}^u&=E\left[\left|\tilde{\mathbf{w}}^H\left(\sqrt{P_{\max}}\sum_{k=1}^{K}\sqrt{\bar{L}_{sp,k}}\mathbf{h}_k s_k^u(t)+n_s(t)\right)\right|^2\right]\\&=\tilde{\mathbf{w}}^H\left(P_{\max}\sum_{k=1}^{K}\bar{L}_{sp,k}\mathbf{R}_k+\sigma_s^2\mathbf{I}_{N_h}\right)\tilde{\mathbf{w}}.\end{aligned} \tag{34}$$

According to the principle of adaptive BF, the optimal weight vector is to minimize the power contributed by the interference plus noise, while maintaining the maximum gain in the direction of intended user [36]. By considering that the uplink BF weight vector is always normalized as $\left\|\tilde{\mathbf{w}}\right\|_F^2=1$, and

$$\tilde{\mathbf{w}}^H\mathbf{R}_s\tilde{\mathbf{w}}=\frac{\tilde{\mathbf{w}}^H\mathbf{R}_s\tilde{\mathbf{w}}}{\tilde{\mathbf{w}}^H\tilde{\mathbf{w}}}\le\lambda_{\max}, \tag{35}$$

where $\lambda_{\max}$ is the maximal eigenvalue of $\mathbf{R}_s$, an optimization problem can be formulated to calculate $\tilde{\mathbf{w}}$ as

$$\min_{\tilde{\mathbf{w}}}\ \tilde{\mathbf{w}}^H\left(P_{\max}\sum_{k=1}^{K}\bar{L}_{sp,k}\mathbf{R}_k+\sigma_s^2\mathbf{I}_{N_h}\right)\tilde{\mathbf{w}}, \tag{36a}$$
$$s.t.\ \bar{L}_s\tilde{\mathbf{w}}^H\mathbf{R}_s\tilde{\mathbf{w}}\le\lambda_{\max}, \tag{36b}$$
$$s.t.\ \ \left\|\tilde{\mathbf{w}}\right\|_F^2=1. \tag{36c}$$

To solve the above optimization problem, the Lagrangian function can be employed and written as

$$\begin{aligned}L(\mathbf{w},\mu)=\min_{\tilde{\mathbf{w}}}\tilde{\mathbf{w}}^H\left(P_{\max}\sum_{k=1}^{K}\bar{L}_{sp,k}\mathbf{R}_k+\sigma_s^2\mathbf{I}_{N_h}\right)\tilde{\mathbf{w}}\\+\mu\left(\bar{L}_s\tilde{\mathbf{w}}^H\mathbf{R}_s\tilde{\mathbf{w}}-\lambda_{\max}\right).\end{aligned} \tag{37}$$

After differentiating the above equation with respect to $\tilde{\mathbf{w}}$, we have

$$\frac{\partial L(\tilde{\mathbf{w}},\mu)}{\partial\tilde{\mathbf{w}}}=\left(P_{\max}\sum_{k=1}^{K}\bar{L}_{sp,k}\mathbf{R}_k+\sigma_s^2\mathbf{I}_{N_h}\right)\tilde{\mathbf{w}}+\mu\bar{L}_s\mathbf{R}_s\tilde{\mathbf{w}}. \tag{38}$$

By letting $\frac{\partial L(\tilde{\mathbf{w}},\mu)}{\partial\tilde{\mathbf{w}}}=0$, the optimal BF weight vector is apparently the maximal eigenvector of $\frac{\mathbf{R}_s}{P_{\max}\sum_{k=1}^{K}\bar{L}_{sp,k}\mathbf{R}_k+\sigma_s^2\mathbf{I}_N}$,

namely,

$$\tilde{\mathbf{w}}_{\text{opt}} = \max .\text{eigenvector}\left(\frac{\bar{L}_s \mathbf{R}_s}{P_{\max}\sum_{k=1}^{K}\bar{L}_{sp,k}\mathbf{R}_k + \sigma_s^2 \mathbf{I}_N}\right). \tag{39}$$

In section VI, we will confirm the validity of the proposed BF scheme through computer simulations. By letting the optimal BF weight vector in (32a) as

$$\mathbf{w}_{opt} = \tilde{\mathbf{w}}_{opt}, \tag{40}$$

and substituting it into the constraint (32b) as

$$P_{th,k} = \frac{Q_k}{\mathbf{w}_{opt}^H \left(\ln\left(\frac{1}{p_{out}}\right)\mathbf{R}_k\right)\mathbf{w}_{opt}}. \tag{41}$$

The allowable transmit power satisfying the interference probability at the BS is given by

$$P_b = \min\left(P_{\max}, P_{th,1}, P_{th,2}, \ldots, P_{th,K},\right). \tag{42}$$

Furthermore, by using (40) and (42) into (27), the output SINR of SU can be further rewritten as

$$\gamma_s = \frac{P_b \bar{L}_s \left|\mathbf{w}_{opt}^H \mathbf{h}_s\right|^2}{P_s \bar{L}_{ps}\left|g_s\right|^2 + \sigma_s^2} = \frac{\bar{\gamma}_b \left|\mathbf{w}_{opt}^H \mathbf{h}_s\right|^2}{\bar{\gamma}_s \left|g_s\right|^2 + 1} = \frac{X}{Y+1}, \tag{43}$$

where $X = \bar{\gamma}_b \left|\mathbf{w}_{opt}^H \mathbf{h}_s\right|^2$ and $Y = \bar{\gamma}_s \left|g_s\right|^2$ with $\bar{\gamma}_b = P_b \bar{L}_s / \sigma_s^2$ and $\bar{\gamma}_s = P_s \bar{L}_{ps} / \sigma_s^2$ being the average SNRs, respectively.

Remark 1: Different from the proposed BF schemes in [21]–[24], where the ULAs and instantaneous CSI are adopted, here we consider the scenarios with UPAs, statistical CSI, and duality of the uplink and downlink.

IV. STATISTICAL PROPERTIES OF SATELLITE AND TERRESTRIAL LINKS

In this section, we provide the statistical properties for both the interference satellite link and desired terrestrial link in (41), which will be used in the subsequent sections for the derivation of the analytical expressions of secondary terrestrial user.

A. SATELLITE LINKS

According to [33], the probability density function of $\left|g_s\right|^2$, for the log-normal fading distribution is

$$f_{|g_s|^2}(x) = \frac{1}{\sqrt{2\pi}\nu_s x}\exp\left(-\frac{\left(\ln x - \mu_s\right)^2}{2\nu_s^2}\right). \tag{44}$$

However, since that shadow fading is very difficult to be characterized by using the lognormal distribution, the expression in (44) is quite complicated and mathematically untractable, making further analysis very complicated. In this paper, we introduce the gamma approximation of the log-normal PDF justified in [37], which means the log-normal PDF of $Y = \bar{\gamma}_s \left|g_s\right|^2$ can be approximated as

$$f_Y(x) \approx \frac{x^{m_s-1}}{\Gamma(m_s)}\left(\frac{m_s}{\Omega_s \bar{\gamma}_s}\right)^{m_s}\exp\left(-\frac{m_s}{\Omega_s \bar{\gamma}_s}x\right), \tag{45}$$

where the parameters m_s and Ω_s are, respectively, given by

$$m_s = \frac{1}{\exp(\sigma_s) - 1}, \text{ and } \Omega_s = q_s\sqrt{\frac{(m_s+1)}{m_s}}, \tag{46}$$

where q_s is the constant area mean power and given by

$$q_s = \exp(\mu_s). \tag{47}$$

B. TERRESTRIAL LINKS

In this paper, by using the well-known Kronecker model [38], [39], the terrestrial channel vector $\mathbf{h}_s$ can be expressed as

$$\mathbf{h}_s = \mathbf{R}_s^{1/2}\tilde{\mathbf{h}}_s. \tag{48}$$

Besides, $\tilde{\mathbf{h}}_s = [\tilde{h}_{s,1}, \tilde{h}_{s,2}, \ldots, \tilde{h}_{s,N}]^T$ with each element being the independent and identically distributed (i.i.d) complex Gaussian random variables (RVs), i.e., $\tilde{h}_{s,j} \sim \mathcal{N}_C(0,1)$, $(j = 1, 2, ..., N)$. By using (40) and (48), X in (43) can be written as

$$\begin{aligned} X &= \bar{\gamma}_b \left|\mathbf{w}_{\text{opt}}^H \mathbf{h}_s\right|^2 \\ &= \bar{\gamma}_b \mathbf{h}_s^H \mathbf{w}_{\text{opt}} \mathbf{w}_{\text{opt}}^H \mathbf{h}_s \\ &= \bar{\gamma}_b \tilde{\mathbf{h}}_s^H \underbrace{\mathbf{R}_s^{\frac{H}{2}} \mathbf{w}_{\text{opt}} \mathbf{w}_{\text{opt}}^H \mathbf{R}_s^{\frac{1}{2}}}_{\Phi} \tilde{\mathbf{h}}_s, \end{aligned} \tag{49}$$

where the non-negative definite matrix Φ can be eigen-decomposed as

$$\Phi = \mathbf{R}_s^{\frac{H}{2}} \mathbf{w}_{opt} \mathbf{w}_{opt}^H \mathbf{R}_s^{\frac{1}{2}} = \mathbf{P}\mathbf{Q}\mathbf{P}^H, \tag{50}$$

where $\mathbf{P} = \left[\mathbf{p}_1, \mathbf{p}_2, \ldots, \mathbf{p}_N\right] \in \mathbb{C}^{N\times N}$ and $\mathbf{Q} = diag(\lambda_1, \lambda_2, \ldots, \lambda_N) \in \mathbb{C}^{N\times N}$ with λ_j $(j = 1, 2, ..., N)$ being the the eigenvalues of $\mathbf{R}_s$ in a non-increasing order, namely, $\lambda_1 \geq \lambda_2 \geq \ldots \geq \lambda_N$, and $\mathbf{p}_j \in \mathbb{C}^{N\times 1}$ the corresponding eigenvectors. By applying the Laplace transform, the PDFs of X can be respectively written as [41]

$$f_X(x) = \sum_{m=1}^{t}\sum_{n=1}^{v_m} \frac{C_{m,n} x^{n-1}}{\Gamma(n)\left(\lambda_m \bar{\gamma}_b\right)^n}\exp\left(-\frac{x}{\lambda_m \bar{\gamma}_b}\right), \tag{51}$$

where the coefficients are given by

$$C_{m,n} = \frac{\left(\lambda_m \bar{\gamma}_b\right)^{j-\nu}}{(v_m - n)!}\frac{\partial^{v_m - n}}{\partial s^{v_m - n}}\left[\prod_{k=1,k\neq m}^{t}\frac{1}{1+\lambda_m \bar{\gamma}_b}\right]\Bigg|_{s=\frac{-1}{\lambda_m \bar{\gamma}_b}}, \tag{52}$$

where t denotes the number of distinct non-zero eigenvalues, v_m the repeated times of λ_m satisfying $\sum_{m=1}^{t} v_m = N$, and $\Gamma(x) = \int_0^\infty \exp(-t)\, t^{x-1} dt$ the Gamma function [40].

V. PERFORMANCE LIMITS ANALYSIS

This section focuses on the performance limits of the cognitive cellular network with the proposed schemes by deriving analytical expressions for outage probability, ergodic capacity, and asymptotic results at high SNR, to well understand the performance limits of the secondary cellular networks.

A. OUTAGE PROBABILITY

The outage probability is an important quality-of-service (QoS) measure in wireless systems and is defined as the probability that the output instantaneous SINR γ_s falls below an acceptable SINR threshold γ_{th}, namely, [6], [18]

$$\Pr\left(\gamma_s \le \gamma_{th}\right) = F_{\gamma_s}\left(\gamma_{th}\right), \tag{53}$$

where $F_{\gamma_s}(x)$ is the cumulative distributed function (CDF) of γ_s. Based on the conditional probability theory, $F_{\gamma_s}(x)$ can be derived as

$$F_{\gamma_s}(x) = \Pr\left(\frac{X}{Y+1} \le x\right) = \int_0^\infty F_X\left[x\left(y+1\right)\right] f_Y(y)\, dy, \tag{54}$$

where $F_X(x)$ is the CDF of X, which can be obtained by using (51) and [40, eq. (3.351.1)] as

$$F_X(x) = 1 - \sum_{m=1}^{t}\sum_{n=1}^{v_m}\sum_{k=0}^{n}\frac{C_{m,n}}{\Gamma(k)}\left(\frac{x}{\lambda_m\bar{\gamma}_b}\right)^k e^{\frac{-x}{\lambda_m\bar{\gamma}_b}}. \tag{55}$$

Then, by substituting (45) and (55) into (54) and performing algebraic manipulations, $F_{\gamma_s}(x)$ can be further expressed as (56), as shown at the bottom of this page. Eventually, replacing the x with γ_{th} in (53), one can directly evaluate the OP of the cognitive terrestrial SU.

B. ERGODIC CAPACITY

The average ergodic capacity is defined as the expected value of the instantaneous mutual information of the received SNR γ_s, namely [6], [21]

$$C_s = E\left[\log_2\left(1+\gamma_s\right)\right] = \int_0^\infty \log_2\left(1+x\right) f_{\gamma_s}(x)\, dx. \tag{57}$$

Applying the integration by parts approach, (57) can be further rewritten as (58), shown at the bottom of this page. Then, by plugging (56) into (58), the analytical expression of C_s can be computed as (59), shown at the bottom of this page.

For the convenience of subsequent derivations, we employ the following identity [41, eq. (11)]

$$\left(1+\alpha x\right)^{-\beta} = \frac{1}{\Gamma(\beta)} G_{1,1}^{1,1}\left[\alpha x \,\middle|\, \begin{matrix} -\beta+1 \\ 0 \end{matrix}\right], \tag{60}$$

reexpressed the $(1+x)^{-1}$ and $\left(\frac{x}{\lambda_m\bar{\gamma}_b}+\frac{m_s}{\Omega_s\bar{\gamma}_s}\right)^{-(j+m_s)}$ in integral I in (59) in terms of the Meijer-G function as

$$\left(1+x\right)^{-1} = G_{1,1}^{1,1}\left[x \,\middle|\, \begin{matrix} 0 \\ 0 \end{matrix}\right], \tag{61}$$

$$\left(\frac{x}{\lambda_m\bar{\gamma}_b}+\frac{m_s}{\Omega_s\bar{\gamma}_s}\right)^{-(j+m_s)} = \frac{1}{\Gamma\left(j+m_s\right)}\left(\frac{m_s}{\Omega_s\bar{\gamma}_s}\right)^{-(j+m_s)} \times G_{1,1}^{1,1}\left[\frac{\Omega_s\bar{\gamma}_s x}{m_s\lambda_m\bar{\gamma}_b} \,\middle|\, \begin{matrix} -\left(j+m_s\right)+1 \\ 0 \end{matrix}\right]. \tag{62}$$

Hence, by utilizing (61) and (62) into (59), we can calculate the integral I as (63), shown at the bottom of the next page, where $G_{1,[1:1],1,[1:1]}^{1,1,1,1,1}[\cdot|\cdot]$ denotes the Meijer-G function of two variables [42]. In deriving (60), we have used [42, eq. (3.1)]. To this end, by substituting (63) into (59), the ergodic capacity C_s of the terrestrial SU can be calculated as

$$C_s = \frac{1}{\ln 2}\sum_{m=1}^{t}\sum_{n=1}^{v_m}\sum_{k=0}^{n}\sum_{j=0}^{k}\binom{k}{j}\frac{C_{m,n}\lambda_m\bar{\gamma}_b}{\Gamma(k)\,\Gamma\left(m_s\right)}\left(\frac{\Omega_s\bar{\gamma}_s}{m_s}\right)^j \times G_{1,[1:1],1,[1:1]}^{1,1,1,1,1}\left[\begin{matrix} \frac{\Omega_s\bar{\gamma}_s}{m_s} \\ \lambda_m\bar{\gamma}_b \end{matrix} \,\middle|\, \begin{matrix} k+1 \\ -\left(j+m_s\right)+1;0 \\ -- \\ 0;0 \end{matrix}\right]. \tag{64}$$

C. ASYMPTOTIC ANALYSIS AT HIGH SNR

Although (56) and (64) are exact and valid for any given SNR, it is unable to provide further insight, such as the effect

$$F_{\gamma_s}(x) = 1 - e^{\frac{-x}{\lambda_m\bar{\gamma}_b}}\sum_{m=1}^{t}\sum_{n=1}^{v_m}\sum_{k=0}^{n}\sum_{j=0}^{k}\binom{k}{j}\frac{C_{m,n}}{\Gamma(k)\,\Gamma\left(m_s\right)}\left(\frac{m_s}{\Omega_s\bar{\gamma}_s}\right)^{m_s}\left(\frac{x}{\lambda_m\bar{\gamma}_b}\right)^k\left(j+m_s-1\right)!\left(\frac{x}{\lambda_m\bar{\gamma}_b}+\frac{m_s}{\Omega_s\bar{\gamma}_s}\right)^{-(j+m_s)}. \tag{56}$$

$$C_s = \log_2\left(1+x\right)\left[F_{\gamma_s}(x)-1\right]_0^\infty - \frac{1}{\ln 2}\int_0^\infty \frac{1}{1+x}\left[F_{\gamma_s}(x)-1\right]dx = \frac{1}{\ln 2}\int_0^\infty \frac{1}{1+x}\left[1-F_{\gamma_s}(x)\right]dx. \tag{58}$$

$$C_s = \frac{1}{\ln 2}\sum_{m=1}^{t}\sum_{n=1}^{v_m}\sum_{k=0}^{n}\sum_{j=0}^{k}\binom{k}{j}\frac{C_{m,n}\left(j+m_s-1\right)!}{\Gamma(k)\,\Gamma\left(m_s\right)\left(\lambda_m\bar{\gamma}_b\right)^k}\left(\frac{m_s}{\Omega_s\bar{\gamma}_s}\right)^{m_s}\underbrace{\int_0^\infty \frac{x^k}{1+x}e^{\frac{-x}{\lambda_m\bar{\gamma}_b}}\left(\frac{x}{\lambda_m\bar{\gamma}_b}+\frac{m_s}{\Omega_s\bar{\gamma}_s}\right)^{-(j+m_s)}dx}_{I}. \tag{59}$$

of channel parameters on the system performance. In this subsection, we provide the asymptotic analysis of OP at high SNR for the cognitive terrestrial network and thereby reveal two important performance merits: diversity order and array gain to obtain further insights into the considered network.

To begin with, applying the MacLaurin series expansion for the exponential function in (55) as [40, eq. (9.303)]

$$F_X^{\infty}(x) = \frac{x}{\bar{\gamma}_b} \sum_{m=1}^{t} \sum_{n=1}^{v_m} \sum_{k=0}^{n} \binom{N}{k} \frac{(-1)^{N-k+1} C_{m,n}}{\lambda_m}. \quad (65)$$

Using (65) and (45) into (54), and with the help of [41, eq.(3.351.3)], the asymptotic expressions of OP in high SNR region can be given by (66), as shown at the bottom of this page.

Then, we express the asymptotic OP expression in (66) into a general form with respective to the diversity order and array gain, namely

$$P_{out}^{\infty}(\gamma_{th}) \approx \Upsilon \left(\frac{\gamma_{th}}{\bar{\gamma}_b} \right) = (G_c \bar{\gamma}_b)^{-G_d}, \quad (67)$$

where

$$G_d = 1, \ and \ \ G_c = \Upsilon^{-1} \Big/ \gamma_{th}, \quad (68)$$

with Υ being given by

$$\Upsilon = \sum_{m=1}^{t} \sum_{n=1}^{v_m} \sum_{k=0}^{n} \binom{N}{k} \frac{(-1)^{N-k+1} C_{m,n}}{\lambda_m} \left(\Omega_s \bar{\gamma}_s + 1 \right). \quad (69)$$

It is revealed in (67) that with the proposed BF schemes, which form a concentrated and directed beam pattern for the desired SU and dampen signals in undesired directions for the PUs, although the diversity order remains one, a significant array gains can be obtained, thereby providing increased SNR for SU. Furthermore, it should be noted that due to the existence of the interference protection at PUs, the OP performance becomes saturated in high SNR regime, which means only zero diversity can be achieved. This is because the interference temperature constraint Q becomes a dominant factor to determine the maximum available transmit power at BS in the case of high $P_{\max}$.

TABLE 1. ITU Recommendation I/N [44],[45].

Interference Pattern	Percentage	Q_k value (dB)
"short term case a)"	0.03% per month	-2.4
"short term case b)"	0.005% per month	0
"long term"	20% per month	-10

VI. NUMERICAL RESULTS

In this section, we provide numerical simulations to confirm the validity of the proposed BF scheme and theoretical derivations, and demonstrate the impact of various parameters on the performance of terrestrial user. Since that the minimum elevation angle for the GEO receivers is commonly adopted around $\alpha_{\min} \approx 10^{\circ}$ to tackle the geographical terrain effect [43]. Without loss of generality, in this paper, we consider the equal elevation and azimuth angles for these K PUs, namely, $\alpha_{s,k} = \alpha$, $\vartheta_{s,k} = \vartheta$, and $Q_k = Q$, $\forall k \in \mathcal{K}$, for the purpose of clear presentation and mathematical simplicity [22], [23]. The horizontal and vertical 3dB beamwidths are set as $\theta_{3dB} = 60^{\circ} \sim 70^{\circ}$ and $\phi_{3dB} = 8^{\circ} \sim 15^{\circ}$ [25], [26]. Table 1 shows the ITU Recommendation for the interference threshold Q at broadband satellite communications in terms of the "short term" and "long term" criteria. Specially, the "short term" criteria can be interpreted in two cases, namely, case a) the received interference at the satellite receivers should not cause the bit error rate to exceed 10^{-4} for more than 0.03% of any month, and case b) the interference should not cause the bit error rate to exceed 10^{-3} for 0.005% of any month. For these percentage of time, the corresponding values of the interference thresholds equal to -2.4 dB and 0 dB, respectively [44]. While for the "long term" criteria, the recommended interference level equals to 10% clear-sky satellite noise that cause a bit error rate of 10^{-6}, and the corresponding value equals to -10 dB [45]. In addition, the simulation results are obtained by performing 10^6 channel realizations, and other parameters are provided in Tables 2 and 3, shown at the top of the next page.

$$\begin{aligned} I &= \frac{1}{\Gamma(j+m_s)} \left(\frac{m_s}{\Omega_s \bar{\gamma}_s} \right)^{-(j+m_s)} \int_0^{\infty} x^k \exp\left(-\frac{x}{\lambda_m \bar{\gamma}_b} \right) G_{1,1}^{1,1}\left[x \middle| \begin{matrix} 0 \\ 0 \end{matrix} \right] \times G_{1,1}^{1,1}\left[\frac{\Omega_s \bar{\gamma}_s x}{m_s \lambda_m \bar{\gamma}_b} \middle| \begin{matrix} -(j+m_s)+1 \\ 0 \end{matrix} \right] dx \\ &= \frac{(\lambda_m \bar{\gamma}_b)^{k+1}}{\Gamma(j+m_s)} \left(\frac{m_s}{\Omega_s \bar{\gamma}_s} \right)^{-(j+m_s)} G_{1,[1:1],1,[1:1]}^{1,1,1,1,1} \left[\begin{matrix} \frac{\Omega_s \bar{\gamma}_s}{m_s} \\ \lambda_m \bar{\gamma}_b \end{matrix} \middle| \begin{matrix} k+1 \\ -(j+m_s)+1; 0 \\ -- \\ 0; 0 \end{matrix} \right]. \end{aligned} \quad (63)$$

$$\begin{aligned} F_{\gamma_s}^{\infty}(x) &= \frac{x}{\Gamma(m_s)\bar{\gamma}_b} \left(\frac{m_s}{\Omega_s \bar{\gamma}_s} \right)^{m_s} \sum_{m=1}^{t} \sum_{n=1}^{v_m} \sum_{k=0}^{n} \binom{N}{k} \frac{(-1)^{N-k+1} C_{m,n}}{\lambda_m} \int_0^{\infty} (y+1) y^{m_s-1} \exp\left(-\frac{m_s}{\Omega_s \bar{\gamma}_s} y \right) dy \\ &= \frac{x}{\bar{\gamma}_b} \sum_{m=1}^{t} \sum_{n=1}^{v_m} \sum_{k=0}^{n} \binom{N}{k} \frac{(-1)^{N-k+1} C_{m,n}}{\lambda_m} \left(\Omega_s \bar{\gamma}_s + 1 \right). \end{aligned} \quad (66)$$

TABLE 2. Simulation Parameters [1],[22],[23],[31].

Orbit	GEO
Frequency band f_c	38 GHz
Bandwidth	500 MHz
Rain fading attenuation (μ_s,ν_s)	(-2.6 dB,1.6 dB)
Maximum BS transmit power	40 dBm
BS antenna height h_{BS}	10 m
PU antenna height $h_{PU,k}$	5 m
SU antenna height h_{SU}	1.5 m
BS antenna main lobe gain $G_{\max}$	17 dB
Front back ratio A_m	25 dB
Side-lobe level limit SLA_V	30 dB
SAT transmit power	30 W
PU antenna main lobe gain $G^P_{\max}$	42.1 dB
Noise temperature	300 K
Free space loss of SAT links	210 dB
Path loss exponents (ξ,β,χ)	(118.77, 0.12, 5.78)
SAT 3-dB beamwidth (φ_{3dB})	0.4°
Angle between SAT beam center and SU (φ_s)	$0.3^\circ \sim 0.8^\circ$
Outage threshold at SU γ_{th}	0 dB
Interference probability constraint p_{out}	0.001
Angular spread of terrestrial links	5°
Number of PUs	3
BS array	8×4, 10×4 UPAs

TABLE 3. Position parameters of SU and PUs [23].

SU's position	$(x_s, y_s, \Delta z_s) = (0.049, 0.0043, -0.0085)\,(Km)$
PUs' position	$(x_1, y_1, \Delta z_1) = (0.707, -0.707, -0.005)\,(Km)$ $(x_2, y_2, \Delta z_1) = (0.866, -0.5, -0.005)\,(Km)$ $(x_3, y_3, \Delta z_3) = (0.866, 0.5, -0.005)\,(Km)$

First of all, we illustrate the beampattern of the proposed BF scheme in Fig. 5, where those of zero-forcing (ZF) and maximal ratio transmission (MRT) BF schemes using the perfect instantaneous CSI are also provided for the purpose of comparison. Clearly, although all of the maximal directions of the beampatterns point to the AOD of SU, and beampattern obtained from the proposed BF scheme also produces deep nulls at the AOD of the K PUs, while that employing MRT scheme without suppressing the mutual interference cannot form nulls at the AODs of the K PUs. Besides, compared with the conventional ZF scheme that requires the instantaneous perfect CSI of each link, the proposed BF scheme can achieve a comparable performance with deeper nulls for the AOD of each PU. Since perfect CSI is often rarely available, the proposed BF scheme with statistical CSI would be a more practical assumption with the advantage of low implementation complexity and reduced overhead.

Then, Fig. 6 plots the outage probability of the terrestrial user for different PU's interference threshold Q and BS array configurations. It can be observed that these theoretical results obtained in (57) are in excellent agreement with the Monte Carlo simulations, and the asymptotic curves in (68) match well with the exact curves at high SNR, confirming the accuracy of our theoretical derivations. Due to the existence of interference probability constraint at PUs, we can see that the outage performance first improves with the increase of $P_{\max}$, and then gradually approaches a plateau in high $P_{\max}$ regime, which can be explained by the fact that in the high $P_{\max}$ regime, the value of Q becomes the dominating factor in limiting the available transmit power at the BS. Besides, the system performance of the cognitive cellular network under a "long term" interference constraint is generally inferior to that of the cases with "short term" constraints. This is an expected results since the interference temperature constraint becomes loose, i.e., Q gets larger, the outage saturation floor reduces, and the outage performance of SU improves. Although the diversity order remains one for both UPA configurations, an improved array gains can be obtained with 8×4 configuration, thereby resulting in reduced outage probability for SU. The achievable diversity order of SU for the proposed BF scheme collapses to zero when the outage saturation occurs, which confirms our findings in the

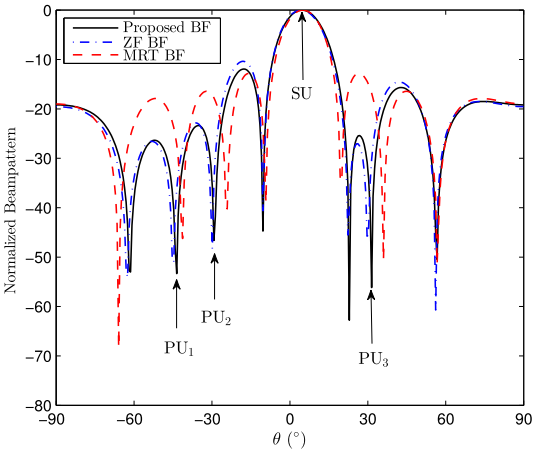

FIGURE 5. Normalized beampattern comparison of proposed BF scheme and conventional BF schemes in horizontal plane ($\alpha = 10°$, $\vartheta = 10°$, $\varphi_s = 0.8$, $\theta_{3dB} = 60°$, $\phi_{3dB} = 8°$), and 8×4 UPA.

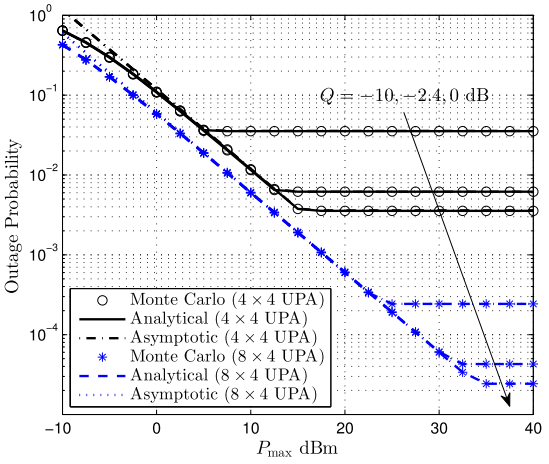

FIGURE 6. Outage probability of the terrestrial SU versus $P_{\max}$ for different values of Q and array configurations with $\alpha = 10°$, $\vartheta = 10°$, $\theta_{3dB} = 60°$, $\phi_{3dB} = 8°$, and $\varphi_s = 0.3$.

asymptotic analysis. Meanwhile, for a fixed Q, the outage saturation of 8×4 UPA occurs at a higher $P_{\max}$ than that of 4×4 UPA. This is because the 8×4 UPA can form deeper nulls to AODs of PUs than that of 4×4 UPA, thus a higher BS transmit power would be tolerable without decorating the operation of PUs.

Fig. 7 depicts the impact of the elevation angle α and azimuth angle ϑ of the BS to PUs interference links on the outage probability of terrestrial SU. Apparently, the interference received at the PUs closely depends on the elevation angle α and ϑ, i.e., larger α and/or ϑ can result in stronger interference from the BS to the PUs. Under this situation, the terrestrial network is required to decrease its transmitting power to alleviate the mutual interference, which will results in a degraded outage performance of the terrestrial network due to the saturation phenomenon for the purpose of PU's normal operation.

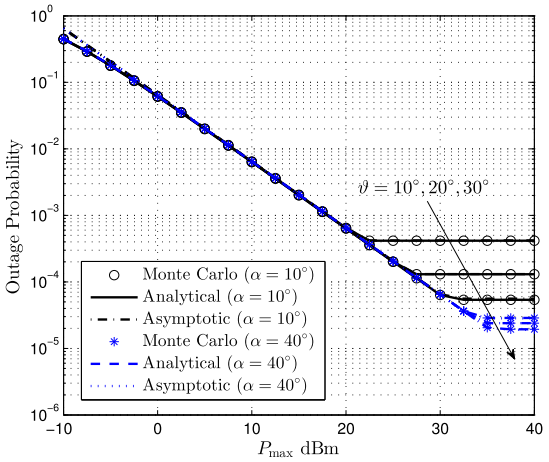

FIGURE 7. Outage probability of the terrestrial SU versus $P_{\max}$ with $Q = -10$ dB, $\theta_{3dB} = 60°$, $\phi_{3dB} = 8°$, $\varphi_s = 0.3$ and 8×4 UPA.

Fig. 8 depicts the ergodic capacity of the terrestrial SU for different interference thresholds Q and SAT beam angle φ_s.

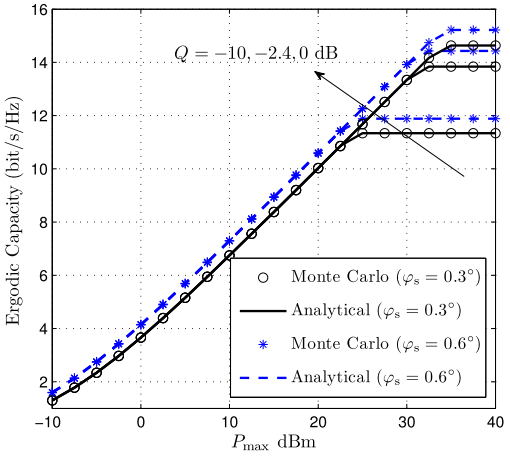

FIGURE 8. Ergodic capacity of the terrestrial SU versus $P_{\max}$ for different values of Q with $\alpha = 10°$, $\vartheta = 10°$, $\theta_{3dB} = 60°$, $\phi_{3dB} = 8°$, and 8×4 UPA.

As we see, the derived analytical expression in (65) is in good agreement with the Monte Carlo simulation results, implying that the derived theoretical formula can accurately evaluate the ergodic capacity of the cognitive network. Again, with the increase of Q, the ergodic capacity gradually increases, indicating that the employment of a stricter interference temperature constraint at the PUs will result in a noteworthy degradation of SU's performance. Meanwhile, the comparison between the beam angle φ_s indicates that the SU with the closer location to the satellite beam center will received a heavier interference from primary satellite network.

Fig. 9 and Fig. 10 show the effect of horizontal and vertical 3dB beamwidths of the BS UPA on the ergodic capacity of terrestrial SU. It can be observed from Fig. 9 that although a larger θ_{3dB} leads to a more interference leakage, the horizontal beamwidth only pose a marginal impact on the ergodic capacity of SU. This is consistent with typical antenna structure, since a large horizontal 3dB beamwidth is relatively preferable to cover a vast region, and thus the effect of its variation is not distinct. While for the vertical

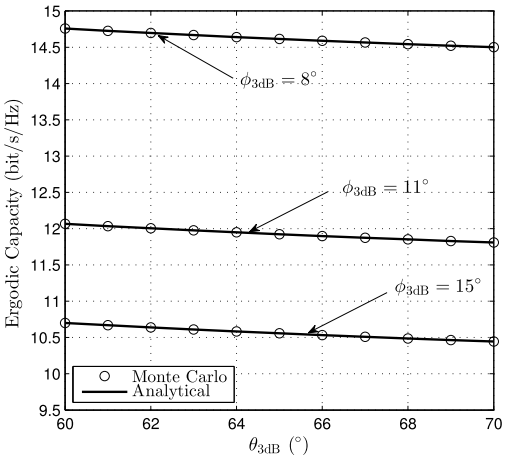

FIGURE 9. Ergodic capacity of the terrestrial SU versus horizontal beamwidth θ_{3dB} with $Q = -10$ dB, $\alpha = 10°$, $\vartheta = 10°$, $\varphi_s = 0.3$, $P_{\max} = 40$ dBm, and 8×4 UPA.

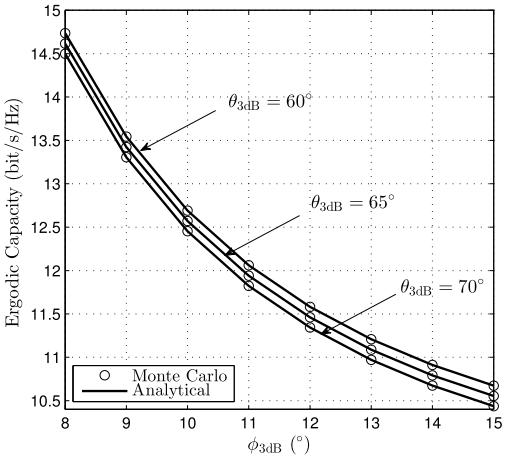

FIGURE 10. Ergodic capacity of the terrestrial SU versus vertical beamwidth ϕ_{3dB} with $Q = -10$ dB, $\alpha = 10°$, $\vartheta = 10°$, $\varphi_s = 0.3$, $P_{\max} = 40$ dBm, and 8×4 UPA.

3dB beamwidths, as shown in Fig. 10, the ergodic capacity of SU significantly decrease with the increase of ϕ_{3dB}. This phenomenon indicates that when vertical BF is applied, the radiation patterns can be further separated, thus prevents extra interference to the primary satellite network.

VII. CONCLUSION

In this paper, we have investigated the performance for the coexistence of broadband satellite system and terrestrial cellular network operating at the mmWave frequency band. By considering the statistical CSI is available, a constrained optimization problem aiming at maximizing the ergodic capacity of the terrestrial user while meeting the interference probability constraint of the PUs has been first formulated. Then, based on a virtual uplink algorithm, the analytical expression for the BF weight vectors and transmit power coefficient are obtained. Furthermore, novel analytical expressions for the outage probability, ergodic capacity, and asymptotic results at high SNR of cognitive terrestrial user are derived. Finally, we provided comprehensive simulation results to justify the validity of the proposed BF scheme and theoretical derivations, and showed the impact of various system parameters on the performance of the terrestrial user.

ACKNOWLEDGMENT

This article was presented in part at the IEEE ICC'2017, Paris, France.

REFERENCES

[1] K. An, M. Lin, J. Guyang, T. Liang, J.-B. Wang, and W.-P. Zhu, "Outage performance for the cognitive broadband satellite system and terrestrial cellular network in millimeter wave scenario," in *Proc. IEEE Int. Conf. Commun. (ICC)*, Paris, France, May 2017, pp. 1–6.

[2] K. An and T. Liang, "Hybrid satellite-terrestrial relay networks with adaptive transmission," *IEEE Trans. Veh. Technol.*, vol. 68, no. 12, pp. 12448–12452, Dec. 2019.

[3] G. Giambene, S. Kota, and P. Pillai, "Satellite-5G integration: A network perspective," *IEEE Netw.*, vol. 32, no. 5, pp. 25–31, Sep./Oct. 2018.

[4] J. G. Andrews, S. Buzzi, W. Choi, S. V. Hanly, A. Lozano, A. C. K. Soong, and J. C. Zhang, "What will 5G be?" *IEEE J. Sel. Areas Commun.*, vol. 32, no. 6, pp. 1065–1082, Jun. 2014.

[5] T. S. Rappaport, S. Sun, R. Mayzus, H. Zhao, Y. Azar, K. Wang, G. N. Wong, J. K. Schulz, M. Samimi, and F. Gutierrez, "Millimeter wave mobile communications for 5G cellular: It will work!" *IEEE Access*, vol. 1, pp. 335–349, May 2013.

[6] K. An, Y. Li, X. Yan, and T. Liang, "On the performance of cache-enabled hybrid satellite-terrestrial relay networks," *IEEE Wireless Commun. Lett.*, vol. 8, no. 5, pp. 1506–1509, Oct. 2019.

[7] J. Du, C. Jiang, H. Zhang, Y. Ren, and M. Guizani, "Auction design and analysis for SDN-based traffic offloading in hybrid satellite-terrestrial networks," *IEEE J. Sel. Areas Commun.*, vol. 36, no. 10, pp. 2202–2217, Oct. 2018.

[8] V. Bankey and P. K. Upadhyay, "Physical layer security of multiuser multirelay hybrid satellite-terrestrial relay networks," *IEEE Trans. Veh. Technol.*, vol. 68, no. 3, pp. 2488–2501, Mar. 2019.

[9] J. Zhang, B. Evans, M. A. Imran, X. Zhang, and W. Wang, "Performance analysis of C/U split hybrid satellite terrestrial network for 5G systems," in *Proc. IEEE 20th Int. Workshop Comput. Aided Modeling Design Commun. Links Netw. (CAMAD)*, Guildford, U.K., Sep. 2015, pp. 97–102.

[10] X. Artiga, A. Perez-Neira, J. Baranda, E. Lagunas, S. Chatzinotas, R. Zetik, P. Gorski, K. Ntougias, D. Perez, and G. Ziaragkas, "Shared access satellite-terrestrial reconfigurable backhaul network enabled by smart antennas at MmWave band," *IEEE Netw.*, vol. 32, no. 5, pp. 46–53, Sep. 2018.

[11] A. K. Gupta, A. Alkhateeb, J. G. Andrews, and R. W. Heath, Jr., "Gains of restricted secondary licensing in millimeter wave cellular systems," *IEEE J. Sel. Areas Commun.*, vol. 34, no. 11, pp. 2935–2950, Nov. 2016.

[12] S. Maleki, S. Chatzinotas, B. Evans, K. Liolis, J. Grotz, A. Vanelli-Coralli, and N. Chuberre, "Cognitive spectrum utilization in ka band multibeam satellite communications," *IEEE Commun. Mag.*, vol. 53, no. 3, pp. 24–29, Mar. 2015.

[13] S. K. Sharma, S. Chatzinotas, and B. Ottersten, "Cognitive radio techniques for satellite communication systems," in *Proc. IEEE 78th Veh. Technol. Conf. (VTC Fall)*, Las Vegas, NV, USA, Sep. 2013, pp. 1–5.

[14] T. Liang, K. An, and S. Shi, "Statistical modeling-based deployment issue in cognitive satellite terrestrial networks," *IEEE Wireless Commun. Lett.*, vol. 7, no. 2, pp. 202–205, Apr. 2018.

[15] X. Yan, H. Xiao, C.-X. Wang, and K. An, "On the ergodic capacity of NOMA-based cognitive hybrid satellite terrestrial networks," in *Proc. IEEE/CIC Int. Conf. Commun. China (ICCC)*, Qingdao, China, Oct. 2017, pp. 1–5.

[16] K. An, M. Lin, J. Ouyang, and W.-P. Zhu, "Secure transmission in cognitive satellite terrestrial networks," *IEEE J. Sel. Areas Commun.*, vol. 34, no. 11, pp. 3025–3037, Nov. 2016.

[17] Y. Ruan, Y. Li, C.-X. Wang, R. Zhang, and H. Zhang, "Effective capacity analysis for underlay cognitive satellite-terrestrial networks," in *Proc. IEEE Int. Conf. Commun. (ICC)*, Paris, France, May 2017, pp. 1–6.

[18] K. An, M. Lin, W.-P. Zhu, Y. Huang, and G. Zheng, "Outage performance of cognitive hybrid satellite–terrestrial networks with interference constraint," *IEEE Trans. Veh. Technol.*, vol. 65, no. 11, pp. 9397–9404, Nov. 2016.

[19] K. Guo, K. An, B. Zhang, Y. Huang, and G. Zheng, "Outage analysis of cognitive hybrid satellite-terrestrial networks with hardware impairments and multi-primary users," *IEEE Wireless Commun. Lett.*, vol. 7, no. 5, pp. 816–819, Oct. 2018.

[20] S. Maleki, S. Chatzinotas, J. Krause, K. Liolis, and B. Ottersten, "Cognitive zone for broadband satellite communications in 17.3–17.7 GHz band," *IEEE Wireless Commun. Lett.*, vol. 4, no. 3, pp. 305–308, Jun. 2015.

[21] K. An, M. Lin, T. Liang, J. Ouyang, and W.-P. Zhu, "On the ergodic capacity of multiple antenna cognitive satellite terrestrial networks," in *Proc. IEEE Int. Conf. Commun. (ICC)*, Paris, France, May 2016, pp. 1124–1128.

[22] F. Guidolin, M. Nekovee, L. Badia, and M. Zorzi, "A study on the coexistence of fixed satellite service and cellular networks in a mmWave scenario," in *Proc. IEEE ICC*, London, U.K., Jun. 2015, pp. 2444–2449.

[23] F. Guidolin, "A cooperative scheduling algorithm for the coexistence of fixed satellite services and 5G cellular network," in *Proc. IEEE ICC*, London, U.K., Jun. 2015, pp. 1322–1327.

[24] S. K. Sharma, S. Chatzinotas, and B. Ottersten, "Transmit beamforming for spectral coexistence of satellite and terrestrial networks," in *Proc. Int. Conf. CROWNCOM*, Jun. 2013, pp. 275–281.

[25] W. Lee, S.-R. Lee, H.-B. Kong, and I. Lee, "3D beamforming designs for single user MISO systems," in *Proc. IEEE Global Commun. Conf. (GLOBECOM)*, Dec. 2013, pp. 3914–3919.

[26] S. M. Razavizadeh, M. Ahn, and I. Lee, "Three-dimensional beamforming: A new enabling technology for 5G wireless networks," *IEEE Signal Process. Mag.*, vol. 31, no. 6, pp. 94–101, Nov. 2014.

[27] C. Liu, W. Feng, Y. Chen, C.-X. Wang, and N. Ge, "Optimal beamforming for hybrid satellite terrestrial networks with nonlinear PA and imperfect CSIT," *IEEE Wireless Commun. Lett.*, vol. 9, no. 3, pp. 276–280, Mar. 2020.

[28] *Reference Radiation Pattern for Earth Station Antennas in the Fixed-Satellite Service for Use in Coordination and Interference Assessment in the Frequency Range from 2 to 31 GHz*, document ITU-R S.465, Jan. 2010.

[29] B. Yu, L. Yang, and H. Ishii, "3D beamforming for capacity improvement in macrocell-assisted small cell architecture," in *Proc. IEEE Global Commun. Conf.*, Austin, TX, USA, Dec. 2014, pp. 4833–4838.

[30] S. K. Yong and J. S. Thompson, "A three-dimensional spatial fading correlation model for uniform rectangular arrays," *IEEE Antennas Wireless Propag. Lett.*, vol. 2, pp. 182–185, 2003.

[31] G. R. MacCartney, Jr., J. Zhang, S. Nie, and T. S. Rappaport, "Path loss models for 5G millimeter wave propagation channels in urban microcells," in *Proc. IEEE GLOBECOM*, Dec. 2013, pp. 3948–3953.

[32] *Prediction Procedure for the Evaluation of Microwave Interference Between Stations on the Surface of the Earth at the Frequencies Above 0.7 GHz*, document ITU-R Recommendation P.452-12, Mar. 2005.

[33] K. An, T. Liang, X. Yan, and G. Zheng, "On the secrecy performance of land mobile satellite communication systems," *IEEE Access*, vol. 6, pp. 39606–39620, Jul. 2018.

[34] A. Kaushik, "On the performance analysis of underlay cognitive radio systems: A deployment perspective," *IEEE Trans. Cognit. Commun. Netw.*, vol. 2, no. 3, pp. 273–287, Sep. 2016.
[35] E. Visotsky and U. Madhow, "Space-time transmit precoding with imperfect feedback," *IEEE Trans. Inf. Theory*, vol. 47, no. 6, pp. 2632–2639, Sep. 2001.
[36] H. L. Van Trees, *Optimum Array Processing*. Hoboken, NJ, USA: Wiley, 2002.
[37] K. An, T. Liang, G. Zheng, X. Yan, Y. Li, and S. Chatzinotas, "Performance limits of cognitive-uplink FSS and terrestrial FS for ka-band," *IEEE Trans. Aerosp. Electron. Syst.*, vol. 55, no. 5, pp. 2604–2611, Oct. 2019.
[38] M. Lin, J. Ouyang, and W.-P. Zhu, "Joint beamforming and power control for device-to-device communications underlaying cellular networks," *IEEE J. Sel. Areas Commun.*, vol. 34, no. 1, pp. 138–150, Jan. 2016.
[39] M. Lin, L. Yang, W.-P. Zhu, and M. Li, "An open-loop adaptive space-time transmit scheme for correlated fading channels," *IEEE J. Sel. Topics Signal Process.*, vol. 2, no. 2, pp. 147–158, Apr. 2008.
[40] I. S. Gradshteyn and I. M. Ryzhik, *Table of Integrals, Series, and Products*, 7th ed. New York, NY, USA: Academic, 2007.
[41] V. S. Adamchik and O. I. Marichev, "The algorithm for calculating integrals of hypergeometric type functions and its realization in reduce systems," in *Proc. Int. Conf. Symp. Algebr. Comput.*, 1990, pp. 212–224.
[42] R. P. Agrawal, "Certain transformation formulae and Meijer's G function of two variables," *Indian J. Pure Appl. Math.*, vol. 1, no. 4, pp. 537–551, 1970.
[43] *Satellite Orbits, Coverage, Antenna Alignment*, Lab-Volt Ltd., Belleville, ON, Canada, 2011.
[44] *Maximum Allowable Values of Interference From Terrestrial Radio Links to Systems in the Fixed-Satellite Service Employing 8-Bit PCM Encoded Telephony and Sharing the Same Frequency Bands*, document ITU-R SF.558-2, Jul. 1986.
[45] *Apportionment of the Allowable Error Performance Degradation to Fixed-Satellite Service (FSS) Hypothetical Reference Digital Paths Arising From Time Invariant Interference for System Operating Below 30 GHz*, document ITU-R Recommendation S.1432, Jan. 2000.

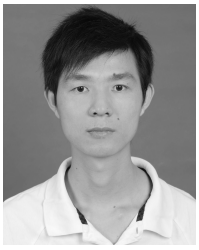

QIANFENG ZHANG received the B.E. and M.S. degrees in mechanical design and theory from Wuhan Textile University, in 2005 and 2008, respectively. Since 2008, he has been with the College of Mechanical, Naval Architecture and Ocean Engineering, Beibu Gulf University, where he is currently an Associate Professor. His current research interests are machine learning, satellite communications, and mechanical design.

KANG AN (Member, IEEE) received the B.E. degree in electronic engineering from the Nanjing University of Aeronautics and Astronautics, Nanjing, China, in 2011, the M.E. degree in communication engineering from the PLA University of Science and Technology, Nanjing, in 2014, and the Ph.D. degree in communication engineering from Army Engineering University, Nanjing, in 2017. Since January 2018, he has been with the National University of Defense Technology, Nanjing, where he is currently an Engineer. His current research interests are satellite communication, 5G mobile communication networks, and cognitive radio.

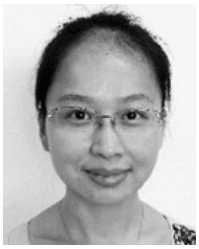

XIAOJUAN YAN (Member, IEEE) received the M.S. degree in control theory and control engineering from Guangxi University, Nanning, China, in 2014, and the Ph.D. degree in information and communication engineering from the Guilin University of Electronic Technology, Guilin, China, in 2019. In 2014, she joined the Beibu Gulf University, where she is currently a Research Associate. She worked as a Visiting Ph.D. Student, under the Supervision of Prof. Cheng-Xiang Wang, at Heriot-Watt University, Edinburgh, U.K., from 2016 to 2017. Her current research interests are in the fields of satellite-terrestrial networks, cooperative communications, non-orthogonal multiple access.

TAO LIANG received the Ph.D. degree in computer science and technology from the Nanjing Institute of Communications Engineering, Nanjing, China, in 1998. He is currently a Research Fellow with the 63rd Research Institute, National University of Defense Technology, and also with the Nanjing Telecommunication Technology Institute, Nanjing. His research interests include satellite communication, digital signal processing in communications, physical layer security, cooperative communication, and cognitive networks.